Nuclear Magnetic Resonance Line-Shape Calculations for a Spin System in a Fixed Lattice*

S. GADE AND I. J. LOWE
Physics Department, University of Pittsburgh, Pittsburgh, Pennsylvania
(Received 7 March 1966)

A theoretical formula is derived for the free-induction decay of a system of identical particles of spin I. The exponential terms containing noncommuting operators are expanded by the method used in the paper by Lowe and Norberg. Only enough terms are kept to make the expansion rigorous through t^4. The resulting formula is evaluated for a system of identical particles for which: (1) the spins form a simple cubic lattice, a face-centered cubic lattice, and a body-centered cubic lattice; (2) there is pure magnetic dipole-dipole interaction between the spins; (3) the applied magnetic field is along the [100], [110], and [111] axes of the lattice; (4) $I=\frac{1}{2}$, 1, $\frac{3}{2}$, and ∞. The Fourier transforms of the free-induction decays are also plotted. The computations show that the free-induction decay shape is remarkably insensitive to the value of I.

I. INTRODUCTION

ONE of the fundamental problems in magnetic resonance is the calculation of the shape of absorption lines in solids. This shape, for a very general set of conditions, is the Fourier transform of the relaxation function $F(t)$ that describes the decay of the component of magnetization that is perpendicular to a steady magnetic field $\mathbf{B}_0$. A general formula for $F(t)$, commonly called the free induction decay (fid), can be readily derived,[1,2] but even a very crude evaluation of the fid is difficult. For the case of a set of spins fixed in spatial position, two attempts have been made to find a general formula for the line shape without making an assumption about the form of the relaxation function or a restriction to a special case such as a system of only two interacting spins. The first of these was by Lowe and Norberg[1] (hereafter referred to as LN), and the second of these was by Clough and McDonald[3] (hereafter referred to as CM). LN derived a general formula for $F(t)$ using an expansion technique that was valid only for spins of angular momentum $I=\frac{1}{2}$ in units of $\hbar$. This formula was evaluated for a system of spins for which (1) the spins formed a simple cubic lattice, (2) there was pure magnetic dipole-dipole interaction between the spins, (3) the applied magnetic field was along the [100], the [110], and the [111] axis of the simple cubic lattice. CM also considered the case of $I=\frac{1}{2}$ only and tried to develop a more general expansion technique. Their formulas were evaluated only for a system of spins for which (1) the spins formed a simple cubic lattice, (2) there was pure magnetic dipole-dipole interaction between the spins, (3) the applied magnetic field was along the [100] axis of the simple cubic lattice. The several different formulas of CM were all as complicated as those of LN and the best agreement between these formulas and experimental results was about as good as those of LN.

In this paper, we use the expansion technique of LN to find the relaxation function $F(t)$ for the case where I may take on any value, and there is dipole-dipole interaction and exchange interaction between the spins. The resulting formulas are evaluated for the cases in which (1) the spins form a simple cubic lattice, a face-centered cubic lattice and a body-centered cubic lattice, (2) there is pure magnetic dipole-dipole interaction between the spins, (3) the applied magnetic field is along the [100], [110], and [111] axes of the lattice, (4) $I=\frac{1}{2}$, 1, $\frac{3}{2}$, and ∞.

II. CALCULATION OF THE FREE-INDUCTION DECAY SHAPE

As stated in the Introduction, the system, whose fid shape we attempt to compute, is a set of N identical particles fixed in space. Each particle has spin I and magnetogyric ratio γ. We assume that there is both dipolar interaction and exchange interaction between the spins. We also assume that this system is in a magnetic field $B_0\hat{z}$ and that this field is large enough that only the terms of the truncated interaction Hamiltonian significantly influence the fid shape.[4] The truncated interaction Hamiltonian $\mathcal{H}$ can be written as follows:

$$\mathcal{H}=\hbar(\alpha+\beta), \tag{1}$$

where

$$\alpha=(1/2\hbar)\sum_{j\neq k}^{N} A_{jk}\mathbf{I}_j\cdot\mathbf{I}_k, \tag{2}$$

$$\beta=(1/2\hbar)\sum_{j\neq k}^{N} B_{jk}I_{jz}I_{kz}, \tag{3}$$

$$B_{jk}=(3\gamma^2\hbar^2/2r_{jk}^3)(1-3\cos^2\theta_{jk}), \tag{4}$$

$$A_{jk}=-\tfrac{1}{3}B_{jk}-2J_{jk}. \tag{5}$$

J_{jk} is the exchange integral between particles j and k. r_{jk} is the distance between particles j and k. θ_{jk} is the

* This work was supported by the U. S. Air Force Office of Scientific Research under Grant No. 196-63. Computations were carried out at the University of Pittsburgh Computing Center, supported in part by the National Science Foundation under Grant No. G11309.

[1] I. J. Lowe and R. E. Norberg, Phys. Rev. **107**, 46 (1957).

[2] A. Abragam, *The Principles of Nuclear Magnetism* (Clarendon Press, Oxford, England, 1961).

[3] S. Clough and I. R. McDonald, Proc. Phys. Soc. (London) **86**, 1 (1965).

[4] J. H. Van Vleck, Phys. Rev. **74**, 1168 (1948).

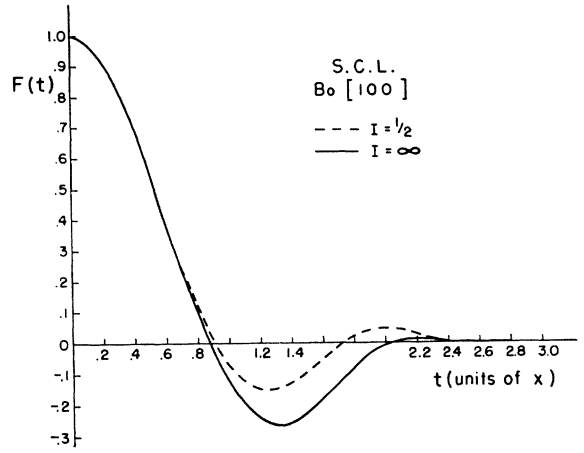

FIG. 1. Free-induction decay shapes for spins in a simple cubic lattice. The applied magnetic field is in the [100] direction and $I=\frac{1}{2}$ and ∞. The fid shapes for $I=1$ and $I=\frac{3}{2}$ lie between the $I=\frac{1}{2}$ and $I=\infty$ fid shapes and are very close to the $I=\infty$ fid shape.

angle between the vector $\mathbf{r}_{jk}$ connecting particles j and k, and the applied magnetic field $B_0\hat{z}$.

The formula for the fid shape, when transformed into the reference frame rotating about the applied magnetic field at a Larmor frequency of $\gamma B_0/2\pi$, is[1,2]

$$F(t)=\frac{\mathrm{Tr}\{I_x\exp(i\mathcal{H}t/\hbar)I_x\exp(-i\mathcal{H}t/\hbar)\}}{\mathrm{Tr}\{I_x^2\}}. \tag{6}$$

Tr{ } signifies that the trace of the operator in the brackets is to be taken, and

$$I_x=\sum_{j=1}^{N} I_{jx}.$$

The evaluation of Eq. (6) is hampered by the many terms in the Hamiltonian $\mathcal{H}$ that do not commute. If the exchange interaction terms are not particularly large, all of the terms in $\mathcal{H}$ are of the same order of magnitude, making a simple perturbation approach difficult. It is easily shown that $[\alpha,I_x]=0$ for all values of I. If $\beta=0$, then $F(t)=1$ and the α term in the Hamiltonian cannot alone influence the fid shape. It is shown in Appendix B that if $\alpha=0$, then $F(t)$ can be easily evaluated exactly. A not unreasonable procedure, therefore, might be to evaluate $F(t)$ exactly for the β term of $\mathcal{H}$ and to treat the α term of $\mathcal{H}$ as a correction term. This is the same technique used by LN for $I=\frac{1}{2}$, and its only justification beyond that given above is the good agreement between these results and the fid shape of fluorine in CaF_2.

With this procedure in mind, we will rewrite Eq. (6) as

$$F(t)=\frac{\mathrm{Tr}\{I_x\exp(i\beta t)\chi^\dagger(t)I_x\chi(t)\exp(-i\beta t)\}}{\mathrm{Tr}I\{_x^2\}} \tag{7}$$

where

$$\chi(t)=\exp(i\alpha t)\exp(-i(\alpha+\beta)t)\exp(i\beta t)$$
$$=\sum_{n=0}^{\infty} C_n t^n/n! \tag{8}$$

and

$$C_n=\partial^n\chi(t)/\partial t^n|_{t=0}. \tag{9}$$

Substituting Eq. (8) into Eq. (7) and combining terms with the same powers of t that derive from $\chi(t)$ yields

$$F(t)=\sum_{n=0}^{\infty} F_n(t)t^n/n!, \tag{10}$$

where

$$F_n(t)=\sum_{p+q=n}\frac{n!\,\mathrm{Tr}\{I_x\exp(i\beta t)C_p^\dagger I_x C_q\exp(-i\beta t)\}}{p!q!\,\mathrm{Tr}\{I_x^2\}}. \tag{11}$$

The first five coefficients of the power series expansion for $\chi(t)$ are

$$C_0=1,\quad C_1=0,\quad C_2=[\alpha,\beta]=\lambda,$$
$$C_3=i[(\alpha-\beta),\lambda],$$
$$C_4=3\lambda^2+[(\beta-\alpha),[\alpha,\lambda]]-[\beta,[\beta,\lambda]].$$

The power series was cut off at t^4 because of the tremendous increase in labor required to evaluate any of the $F_n(t)$ for $n>4$. A comparison of theoretical and experimental results will indicate the range of t for which this procedure is valid.

For the case in which $\alpha=0$, all $C_n=0$ except for C_0 which is equal to 1. Then

$$F(t)=F_0(t).$$

The term $F_0(t)$ is evaluated in Appendix (B) where it is shown that

$$F_0(t)=\frac{1}{N}\sum_{k=1}^{N}\prod_j{}'\left(\frac{\sin((2I+1)B_{jk}t/2\hbar)}{(2I+1)\sin(B_{jk}t/2\hbar)}\right). \tag{12}$$

Equation (12) reduces to the result that LN found for the case $I=\frac{1}{2}$ and $\alpha=0$.

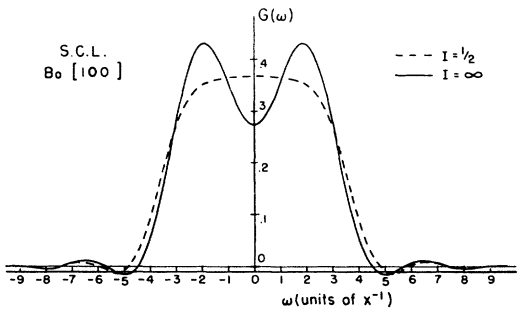

FIG. 2. Absorption curves for spins in a simple cubic lattice. The applied magnetic field is in the [100] direction and $I=\frac{1}{2}$ and ∞. The absorption curves for $I=1$ and $I=\frac{3}{2}$ lie between the $I=\frac{1}{2}$ and $I=\infty$ curves.

Evaluation of the F_2, F_3 and F_4 terms is straightforward but tedious. The method of evaluation of a typical term is shown in Appendix (A). Listed below is the four-term approximation of $F(t)$, that is $F_0(t)+F_2(t)t^2/2!+F_3(t)t^3/3!+F_4(t)t^4/4!$. The listed solution, Eqs. (13)–(16), is for a lattice in which all the nuclei occupy equivalent sites.

$$F(t)=U(t)V(t)\,, \tag{13}$$

$$U(t)=\prod_j{}'\left[\frac{\sin((2I+1)B_{jk}t/2\hbar)}{(2I+1)\sin(B_{jk}t/2\hbar)}\right], \tag{14}$$

$$\begin{aligned}
V(t)=1&+(t^2/2\hbar^2)\{\sum_{n\neq i}{}' A_{pn}(B_{pi}-B_{ni})Z_{ip}(t)Z_{np}(t)+\tfrac{1}{2}\sum_n{}' A_{pn}B_{pn}X_{np}(t)\}\\
&+(t^3/3!\hbar^3)\{\sum_{n\neq i}{}'[(B_{pi}-B_{ni})A_{pn}(A_{pn}-2B_{pn})+(B_{pn}-B_{ni})A_{pi}(A_{np}-B_{np}+B_{ni})\\
&-A_{in}^2(B_{ip}-B_{np})+B_{np}A_{np}A_{ip}]Z_{ip}(t)G_{np}(t)+\sum_{n\neq i}{}'[(B_{pi}-B_{ni})(A_{np}^2+A_{np}A_{ni}+2A_{np}B_{np})\\
&-A_{pi}A_{ni}(B_{np}-B_{ni})+(B_{pi}-B_{pn})(3A_{in}^2+A_{in}A_{pn})-B_{np}A_{np}A_{ip}]Z_{ip}(t)H_{np}(t)\\
&+\sum_n{}' A_{np}^2B_{np}[(\tfrac{3}{5}I(I+1)-7/10)Z_{np}(t)+(D_{np}(t))^{-1}\sum_{m=-I}^{+I} m^3\sin(B_{np}mt/\hbar)]\\
&+\sum_n{}' A_{np}B_{np}^2[(\tfrac{4}{5}I(I+1)-\tfrac{1}{10})Z_{np}(t)-(D_{np}(t))^{-1}\sum_{m=-I}^{+I} 2m^3\sin(B_{np}mt/\hbar)]\}\\
&-(t^4/4!\hbar^4)\{\sum_{n\neq i}{}'[-3A_{np}B_{np}(B_{ni}-B_{pi})^2-A_{ni}^2A_{np}B_{np}+A_{ni}B_{ni}A_{np}^2-3A_{np}B_{np}A_{pi}^2+A_{ni}^2A_{np}B_{ip}\\
&-A_{ni}B_{ni}A_{pi}A_{pn}+2A_{pn}^2B_{ni}A_{ip}-B_{in}^2A_{in}A_{np}+B_{in}^2A_{np}^2-2A_{in}B_{in}A_{ip}B_{ip}+A_{np}^2B_{ip}^2+2A_{np}B_{np}A_{ip}B_{ip}\\
&+2A_{in}B_{in}A_{np}B_{ip}-2A_{np}B_{np}B_{ni}A_{ip}-2A_{np}^2B_{ni}B_{ip}]G_{ip}(t)G_{np}(t)+\sum_{n\neq i}{}'[12A_{ni}^2B_{ni}A_{pi}+11A_{ni}^2A_{np}B_{np}\\
&+2A_{in}B_{in}A_{np}^2+4A_{np}^2A_{pi}B_{pi}-9A_{ni}^2A_{np}B_{ip}-4A_{in}B_{in}A_{ip}A_{pn}-3A_{np}^2B_{ni}A_{ip}+A_{np}B_{np}A_{ip}A_{ni}\\
&-3A_{ip}^2A_{ni}B_{pn}+4A_{ip}^2B_{ip}A_{in}+6B_{ni}^2A_{ni}A_{np}+6A_{ni}^2B_{np}^2+A_{ni}B_{ni}A_{np}B_{np}-6A_{in}^2B_{np}B_{ip}-8A_{in}B_{in}B_{np}A_{ip}\\
&-A_{np}B_{np}A_{ni}B_{ip}+B_{pi}^2A_{np}A_{ni}]H_{np}(t)H_{ip}(t)+\sum_{n\neq i}{}'[3A_{np}B_{np}(B_{ni}-B_{pi})^2-8A_{ni}^2B_{ni}A_{pi}-4A_{ni}^2B_{ni}A_{np}\\
&+A_{ni}^2A_{np}B_{np}-11A_{ni}^2B_{pi}A_{pi}+2A_{in}B_{in}A_{np}^2-5A_{in}B_{in}A_{ip}^2-2A_{np}^2B_{ip}A_{ip}+A_{np}B_{np}A_{ip}^2+2A_{ni}^2A_{np}B_{pi}\\
&+6A_{ni}^2A_{ip}B_{np}+5A_{in}B_{in}A_{ip}A_{pn}+A_{pn}^2B_{ni}A_{ip}-A_{np}^2B_{pi}A_{in}+A_{np}B_{np}A_{pi}A_{ni}+4A_{ip}^2A_{ni}B_{np}\\
&-2A_{ip}B_{ip}A_{pn}A_{ni}-4A_{ip}^2B_{ip}A_{in}-5B_{in}^2A_{in}A_{ip}+2B_{in}^2A_{np}+3B_{ni}A_{ni}A_{np}B_{np}+4A_{ni}B_{ni}A_{ip}B_{ip}\\
&+2A_{np}^2B_{ip}^2-2A_{np}B_{np}B_{ip}A_{ip}-4A_{ni}B_{ni}A_{np}B_{ip}+4A_{ni}B_{ni}A_{ip}B_{np}-4A_{np}^2B_{ni}B_{pi}\\
&+2A_{np}B_{np}B_{ni}A_{ip}-3A_{np}B_{np}B_{ip}A_{ni}+5B_{ip}^2A_{pn}A_{in}-2A_{pi}B_{pi}A_{ni}B_{np}]H_{np}(t)G_{ip}(t)+\tfrac{1}{2}\sum_n{}' B_{np}^3A_{np}\\
&\times[\tfrac{3}{5}I^2(I+1)^2-(7/10)I(I+1)+((6/5)I(I+1)+(11/10))G_{np}(t)-5(D_{np}(t))^{-1}\sum_{m=-I}^{+I} m^4\cos(B_{np}mt/\hbar)]\\
&+\tfrac{1}{2}\sum_n{}' A_{np}^3B_{np}[(32/5)I^2(I+1)^2-(33/10)I(I+1)-((96/5)I(I+1)-(99/10))G_{np}(t)]\\
&+\tfrac{1}{2}\sum_n{}' A_{np}^2B_{np}^2[(18/5)I^2(I+1)^2-(17/10)I(I+1)-((24/5)I(I+1)-\tfrac{1}{10})G_{np}(t)\\
&\qquad+2(D_{np}(t))^{-1}\sum_{m=-I}^{+I} m^4\cos(B_{np}mt/\hbar)]\}\,,
\end{aligned} \tag{15}$$

where

$$\begin{aligned}
&Z_{ip}(t)=\tfrac{1}{2}\cot(B_{ip}t/2\hbar)-(I+\tfrac{1}{2})\cot((I+\tfrac{1}{2})(B_{ip}t/\hbar))\,,\\
&X_{ip}(t)=-2I(I+1)+\tfrac{3}{2}\cot^2(B_{ip}t/2\hbar)-3(I+\tfrac{1}{2})\cot((I+\tfrac{1}{2})(B_{ip}t/\hbar))\cot(B_{ip}t/2\hbar)\,,\\
&H_{ip}(t)=\tfrac{1}{3}I(I+1)+\tfrac{1}{6}X_{ip}(t)\,,\quad G_{ip}(t)=\tfrac{1}{3}I(I+1)-\tfrac{1}{3}X_{ip}(t)\,,
\end{aligned} \tag{16}$$

and

$$D_{ip}(t)=\frac{\sin((I+\frac{1}{2})(B_{ip}t/\hbar))}{\sin(B_{ip}t/2\hbar)}.$$

The primes on the summation and product signs denote that the particle subscripts summed over are not to be taken as equal to the particle subscripts not summed over.

This expression for $F(t)$ yields second and fourth moments that agree with those of Van Vleck's.[4] When I is set equal to $\frac{1}{2}$, the above expression reduces to the expression found by LN.

III. CALCULATION OF THE FREE-INDUCTION DECAY FOR PURE DIPOLAR INTERACTIONS BETWEEN SPINS IN A LATTICE HAVING CUBIC SYMMETRY

For pure dipolar interactions between the spins of the system, $A_{jk}=-\frac{1}{3}B_{jk}$. Equation (15) for $V(t)$ can be reduced to

$$\begin{aligned}V(t)=1&-t^2(/6\hbar^2)\{(\textstyle\sum_n{}' B_{np}Z_{np}(t))^2-\sum_n{}' B_{np}{}^2(Z_{np}(t))^2+\tfrac{1}{2}\sum_n{}' B_{np}{}^2X_{np}(t)\}\\
&+(t^3/54\hbar^3)\{4I(I+1)\textstyle\sum_n{}' B_{np}{}^2\sum_i B_{ip}Z_{ip}(t)-5\sum_n{}' B_{np}Z_{np}(t)\sum_i{}' B_{ip}{}^2X_{ip}(t)\\
&+\textstyle\sum_n{}' B_{np}{}^3[5Z_{np}(t)X_{np}(t)+((6/5)I(I+1)-(39/10))Z_{np}(t)-\frac{7}{2}X_{np}(t)\cot(B_{np}t/2\hbar)]\}\\
&-[t^4/((27)(4!)\hbar^4)]\{6I^2(I+1)^2(\textstyle\sum_n{}' B_{np}{}^2)^2-[16I^2(I+1)^2-(15/2)I(I+1)]\sum_n{}' B_{np}{}^4-(83/6)I(I+1)\\
&\times\textstyle\sum_n{}' B_{np}{}^2\sum_i{}' B_{ip}{}^3X_{ip}(t)+(17/3)(\sum_n{}' B_{np}{}^2X_{np}(t))^2-(17/3)\sum_n{}' B_{np}{}^4(X_{np}(t))^2\\
&-[(13/6)I(I+1)-(81/4)]\textstyle\sum_n{}' B_{np}{}^4X_{np}(t)+(51/2)\sum_n{}' B_{np}{}^4X_{np}(t)\cot^2(B_{np}t/2\hbar)\}. \quad (17)\end{aligned}$$

In evaluating Eq. (17) all summations have been dropped which contain odd functions of B_{jk}. The justification for doing this is that B_{jk} is a function of θ that averages to zero when integrated over a sphere. Therefore, a summation of an odd power of B_{jk} over a cubic lattice will be small in comparison to a summation of an even power of B_{jk}.

Using Eqs. (13), (14), (16), and (17), free-induction decay shapes have been evaluated for the following combinations of situations: (1) simple cubic lattice, body-centered cubic lattice, face-centered cubic lattice, (2) the applied magnetic field is along the [100], [110], and [111] axes of the lattice, (3) $I=\frac{1}{2}$, 1, $\frac{3}{2}$, and ∞. The free induction decay for infinite I is found by letting $I\to\infty$ and $\hbar\to 0$ in Eqs. (14) and (17) in such a way that $\hbar I$ remains finite. In the next section, this limiting case is shown to be equivalent to the results obtained for a set of magnetic dipoles with angular momentum that obeys the classical equations of motion.

In the numerical evaluation of Eqs. (14) and (17), the various terms are left intact for near neighbors. For more distant neighbors, these terms are expanded in a power series of t, the terms having the same powers of t are combined so that lattice sums can be used. The number of nearest neighbors considered exactly are 80 for the simple cubic lattice, 168 for the body-centered cubic lattice, and 200 for the face-centered cubic lattice. The free-induction decays are evaluated as functions of t in units of x, where

$$x=2d^3/3\gamma^2\hbar[I(I+1)]^{1/2},$$

and d is the lattice parameter of the cubic unit cell.

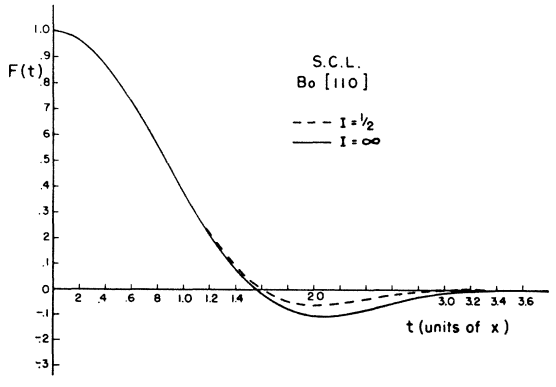

FIG. 3. Free-induction decay shapes for spins in a simple cubic lattice. The applied magnetic field is in the [110] direction and $I=\frac{1}{2}$ and ∞. The fid shapes for $I=1$ and $I=\frac{3}{2}$ lie between the $I=\frac{1}{2}$ and $I=\infty$ fid shapes and are very close to the $I=\infty$ fid shape.

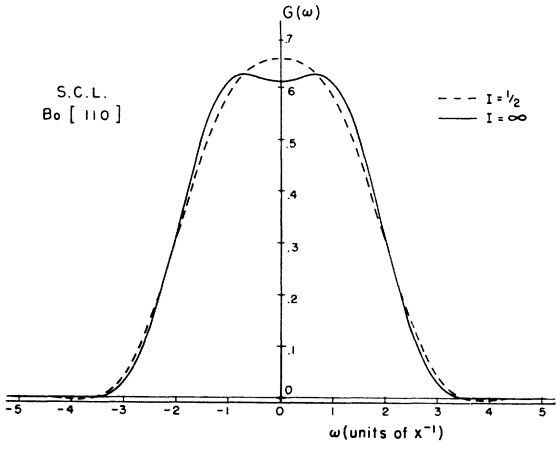

FIG. 4. Absorption curves for spins in a simple cubic lattice. The applied magnetic field is in the [110] direction and $I=\frac{1}{2}$ and ∞. The absorption curves for $I=1$ and $I=\frac{3}{2}$ lie between the $I=\frac{1}{2}$ and $I=\infty$ curves and are very close to the $I=\infty$ curve.

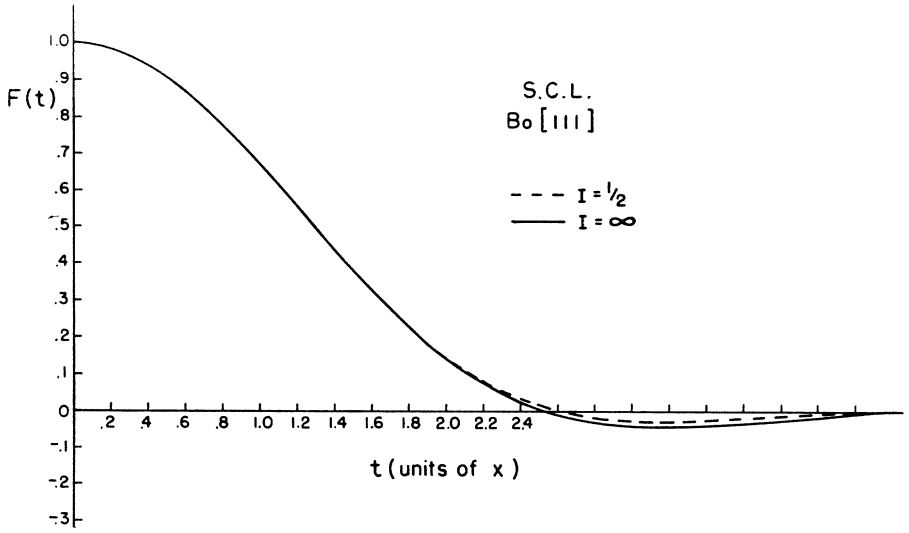

FIG. 5. Free-induction decay shapes for spins in a simple cubic lattice. The applied magnetic field is in the [111] direction and $I=\frac{1}{2}$ and ∞. The fid shapes for $I=1$ and $I=\frac{3}{2}$ lie between the $I=\frac{1}{2}$ and $I=\infty$ fid shapes.

Therefore, d is equal to the distance between nearest neighbors in the simple cubic lattice, and to $2/\sqrt{3}$ times the distance between nearest neighbors in the body-centered cubic lattice, and to $\sqrt{2}$ times the distance between nearest neighbors in the face-centered cubic lattice. The numerical evaluation of the free induction decays $F(t)$ and their Fourier transforms $G(\omega)$ (the absorption curves) were carried out on an IBM 7090 computer. The results are plotted in Figs. 1 to 18.

Some of the absorption curves have small regions over which they are slightly negative. The curve in these regions must be wrong since the absorption curve is a positive quantity. We think this result is due to *small* errors in the free-induction decay shape. When $G(\omega)$ is small for small ω, small errors in the free-induction decay shape have a large effect on the value of $G(\omega)$ because $G(\omega)$ is small for small ω due to the almost exact cancelation of $\int F(t)\cos\omega t dt$ for only one or two oscillations of $\cos\omega t$ in the region where $F(t)$ is large. In Figs. 2, 4, 6, 8, 10, 12, 14, 16, and 18 the light horizontal line is the $G(\omega)=0$ coordinate. The dark horizontal line is the $G(\omega)=-0.01$ coordinate for Figs. 2, 4, 6, 8, 10, and 12, and the $G(\omega)=-0.005$ line for Figs. 14, 16, and 18. The numerical tables on which Figs. 1 to 18 are based can be obtained by writing to the authors.

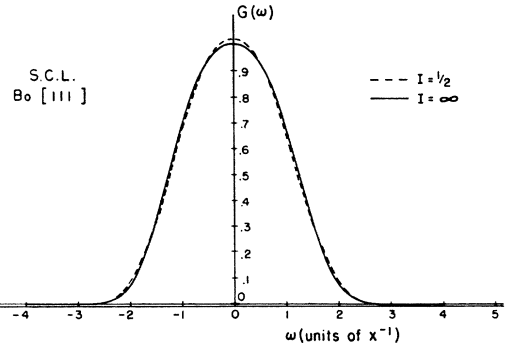

FIG. 6. Absorption curves for spins in a simple cubic lattice. The applied magnetic field is in the [111] direction and $I=\frac{1}{2}$ and ∞. The $I=1$ and $I=\frac{3}{2}$ absorption curves lies between the $I=\frac{1}{2}$ and $I=\infty$ curves.

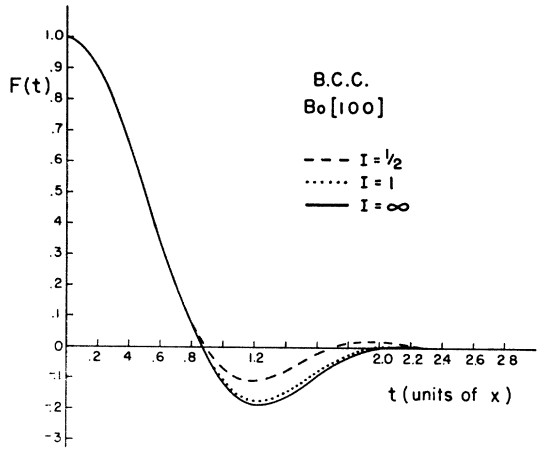

FIG. 7. Free-induction decay shapes for spins in a body-centered cubic lattice. The applied magnetic field is in the [100] direction and $I=\frac{1}{2}$, 1, and ∞. The $I=\frac{3}{2}$ fid shape lies between the $I=1$ and $I=\infty$ fid shapes.

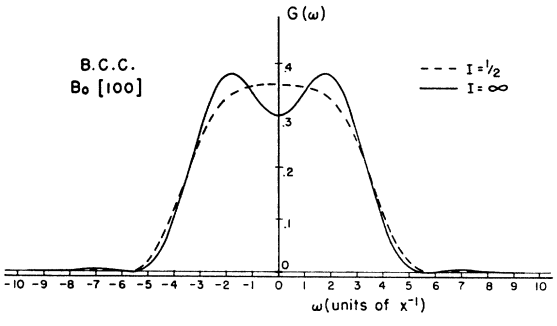

FIG. 8. Absorption curves for spins in a body-centered cubic lattice. The applied magnetic field is in the [100] direction and $I=\frac{1}{2}$ and ∞. The $I=1$ and $I=\frac{3}{2}$ absorption curves lie between the $I=\frac{1}{2}$ and $I=\infty$ absorption curves and are very close to the $I=\infty$ curve.

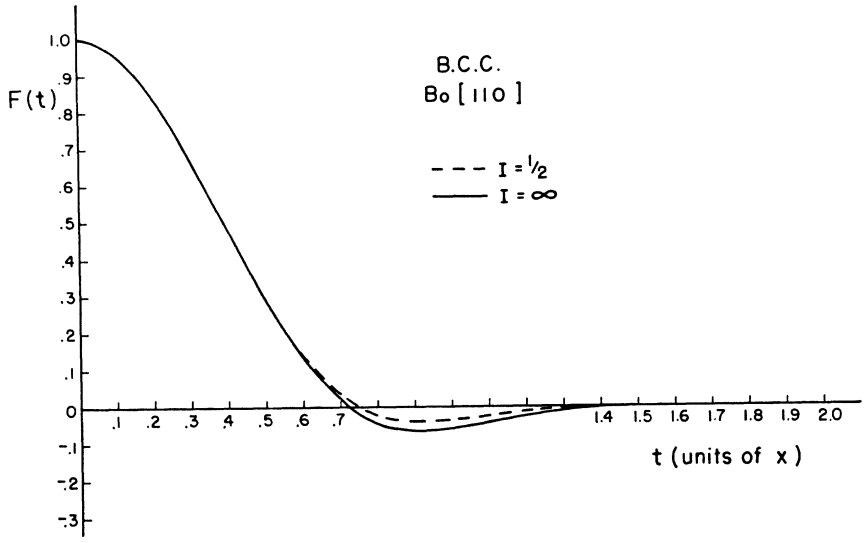

FIG. 9. Free-induction decay shapes for spins in a body-centered cubic lattice. The applied magnetic field is in the [110] direction and $I=\frac{1}{2}$ and ∞. The $I=1$ and $I=\frac{3}{2}$ fid shapes lie between the $I=\frac{1}{2}$ and $I=\infty$ fid shapes and are very close to the $I=\infty$ fid shape.

IV. THE FREE-INDUCTION DECAY SHAPE FOR INFINITE I

As mentioned in the previous section, the formula for the free induction decay shape for infinite I was obtained by taking the limits for Eqs. (14) and (17) for $I\rightarrow\infty$ and $\hbar\rightarrow 0$ such that $\hbar I$ remained finite. For this limit, angular momentum behaves classically. In order to see if there would be some simplification in the line shape calculations for classical angular momentum, formulas for line shapes were computed using classical theory. Several different techniques were attempted and they all produced answers identical to the above discussed limiting case without introducing any new physical insight into the problem.

The simplest of these techniques involved the replacing of commutators by Poisson brackets. Regardless of whether the LN expansion or the moment expansion is used for the function $F(t)$ the results assume the form of a series of terms each of which consists of appropriate spatial variables multiplied by the trace of a commutator containing angular-momentum operators. The corresponding classical solution for the free-induction decay was obtained by replacing all these commutators with Poisson brackets, and by replacing the traces over a complete set of angular-momentum states by a classical average over all directions of the angular-momentum vector. As previously stated, these results are identical to the limiting case of $I\rightarrow\infty$ and $\hbar\rightarrow 0$.

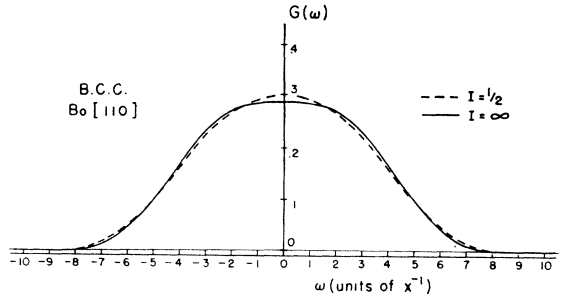

FIG. 10. Absorption curves for spins in a body-centered cubic lattice. The applied magnetic field is in the [110] direction and $I=\frac{1}{2}$ and ∞. The $I=1$ and $I=\frac{3}{2}$ absorption curves lie between the $I=\frac{1}{2}$ and $I=\infty$ absorption curves and are very close to the $I=\infty$ curve.

V. DISCUSSION

The most significant feature of the theoretical curves for the computed free-induction decays in Figs. 1, 3, 5, 7, 9, 11, 13, 15, and 17 is the relatively small dependence

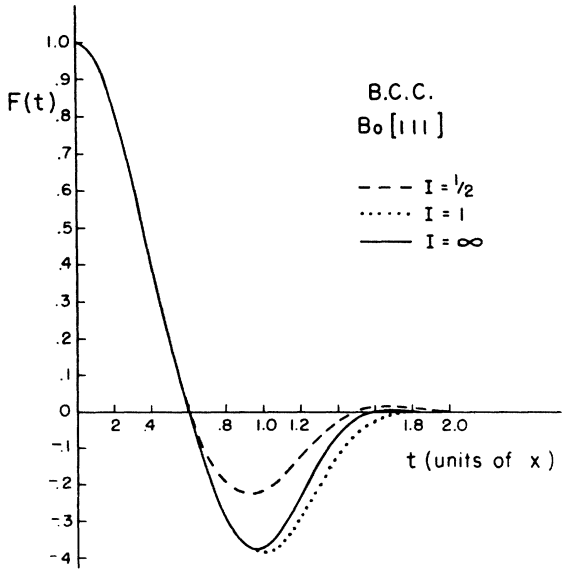

FIG. 11. Free-induction decay shapes for spins in a body-centered cubic lattice. The applied magnetic field is in the [111] direction and $I=\frac{1}{2}$, 1, and ∞. The $I=\frac{3}{2}$ fid shape lies between the $I=1$ and $I=\infty$ fid shapes.

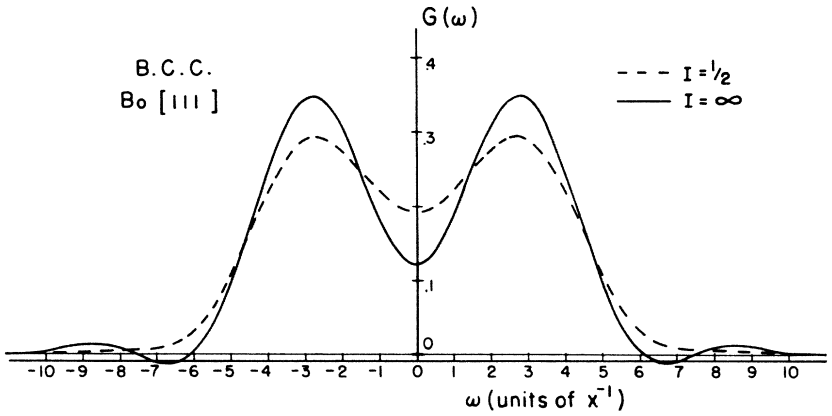

FIG. 12. Absorption curves for spins in a body-centered cubic lattice. The applied magnetic field is in the [111] direction and $I=\frac{1}{2}$ and ∞. The $I=1$ and $I=\frac{3}{2}$ absorption curves lie close to the $I=\infty$ curve.

of the shape of the calculated free-induction decays upon the spin value I for a given crystal symmetry and the direction of the applied magnetic field. These results are somewhat unexpected since the free-induction decay shapes for just two interacting particles is strongly dependent upon the spin value I.

The relative insensitivity of the calculated free induction decay shape upon the value of I can be explained in the following way. The free-induction decay shape $F(t)$ can be expressed in terms of the moments of the absorption line[1,2] by the relationship

$$F(t)=\sum_{n=0}^{\infty}(-1)^n(M_{2n}/M_0)t^{2n}, \tag{18}$$

where M_{2n} is the $2n$th moment of the absorption line. M_{2n} contains terms which involve 2, 3, 4, $\cdots$, $n+1$ particles. For the case of pure dipolar interaction between the particles, it is conjectured that terms involving interactions between $n+1$ particles constitute the largest part of the $2n$th moment.[5] These terms contain traces of products like[5] $I_{jz}^2I_{ky}^2I_{lx}^2\cdots$, which when evaluated are proportional to $(I(I+1))^n$. Thus, to a first approximation one may write

$$F(t)=\sum_{n=0}^{\infty}(-1)^n\xi_n([(I)(I+1)]^{1/2}t)^{2n}, \tag{19}$$

where ξ is independent of I and depends only upon spatial variables and γ. Therefore, the plot of $F(t)$ versus t, where t is taken in units of $x=2d^3/3\gamma\hbar^2(I(I+1))^{1/2}$, is quite insensitive to the value of I.

This analysis may be pushed a little bit further. By expanding Eq. (13) for $F(t)$ in powers of t, we find for pure dipolar interaction between spins, that

$$M_4/M_0=\{3(\textstyle\sum'_k B_{jk}^2)^2-(1/3N)\sum_{j\neq k\neq l}B_{jk}^2(B_{jl}-B_{kl})^2$$
$$-\tfrac{1}{5}\textstyle\sum'_k B_{jk}^4[8+(3/2I(I+1))]\}(I(I+1)/3\hbar^2)^2. \tag{20}$$

The most important terms for determining the shape of $F(t)$ for small t are M_2 and M_4. The M_2 term is proportional to $I(I+1)$ and the only term in M_4 that is not

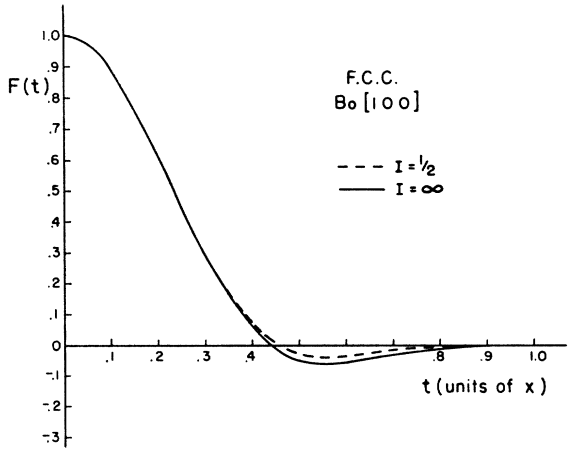

FIG. 13. Free-induction decay shapes for spins in a face-centered cubic lattice. The applied magnetic field is in the [100] direction and $I=\frac{1}{2}$ and ∞. The $I=1$ and $I=\frac{3}{2}$ fid shapes lie between the $I=\frac{1}{2}$ and $I=\infty$ fid shapes and are very close to the $I=\infty$ fid shape.

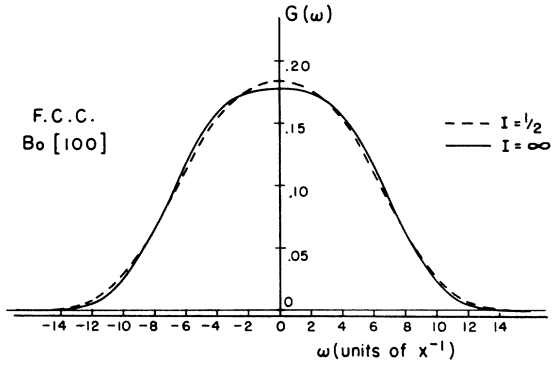

FIG. 14. Absorption curves for spins in a face-centered cubic lattice. The applied magnetic field is in the [100] direction and $I=\frac{1}{2}$ and ∞. The $I=1$ and $I=\frac{3}{2}$ absorption curves lie between the $I=\frac{1}{2}$ and $I=\infty$ absorption curves and are close to the $I=\infty$ curve.

[5] R. Bersohn and T. P. Das, Phys. Rev. **130**, 98 (1963).

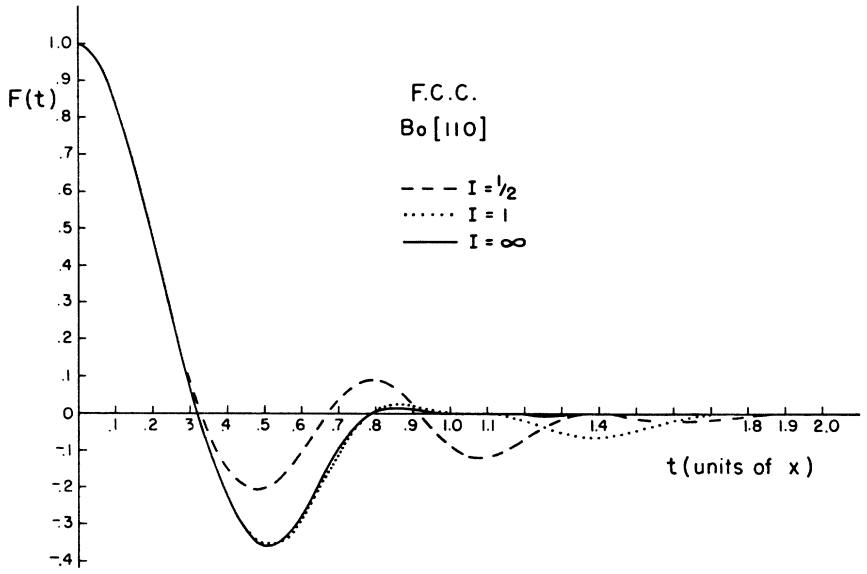

FIG. 15. Free-induction decay shapes for spins in a face-centered cubic lattice. The applied magnetic field is in the [110] direction and $I=\frac{1}{2}$, 1, and ∞. The $I=\frac{3}{2}$ fid shape lies between the $I=1$ and $I=\infty$ fid shapes.

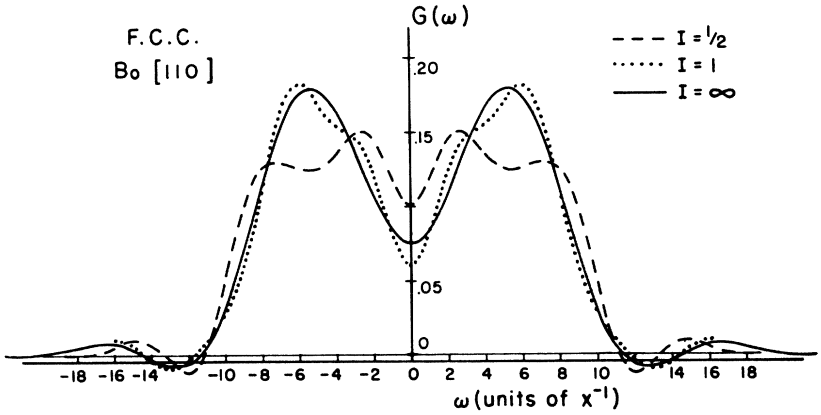

FIG. 16. Absorption curves for spins in a face-centered cubic lattice. The applied magnetic field is in the [110] direction and $I=\frac{1}{2}$, 1, and ∞. The absorption curve for $I=\frac{3}{2}$ lies between the $I=1$ and $I=\infty$ curves.

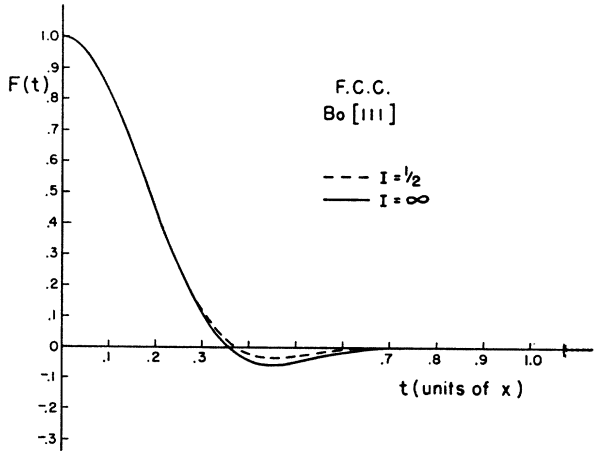

FIG. 17. Free-induction decay shapes for spins in a face-centered cubic lattice. The applied magnetic field is in the [111] direction and $I=\frac{1}{2}$ and ∞. The fid shapes for $I=1$ and $I=\frac{3}{2}$ lie between the $I=\frac{1}{2}$ and $I=\infty$ fid shapes and are close to the $I=\infty$ fid shape.

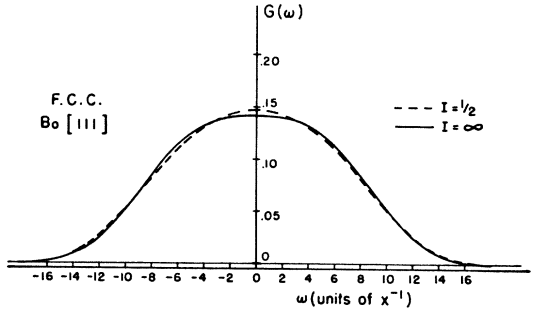

FIG. 18. Absorption curves for spins in a face-centered cubic lattice. The applied magnetic field is in the [111] direction and $I=\frac{1}{2}$ and ∞. The absorption curves for $I=1$ and $I=\frac{3}{2}$ lie between the $I=\frac{1}{2}$ and $I=\infty$ absorption curves.

proportional to $(I(I+1))^2$ is $\sum_k' B_{jk}^4$. Terms with the form $(\sum_k' B_{jk}^2)^2$ make the most important contribution to the fourth moment. Therefore, σ, where

$$\sigma=(\textstyle\sum_k' B_{jk}^2)^2/(\sum_k' B_{jk}^4), \qquad (21)$$

TABLE I. Listing of the crystal symmetry and applied magnetic field direction in order of increasing dependence of the free-induction decay shape upon I. In the third column is the corresponding value of $\sigma=(\sum_j' B_{ij}^2)^2/\sum_j' B_{ij}^4$.

Crystal symmetry	Direction of applied magnetic field	σ
scl	[111]	19.1
fcc	[111]	14.8
fcc	[100]	14.4
bcc	[110]	13.0
scl	[110]	8.9
bcc	[100]	6.3
scl	[100]	4.6
fcc	[110]	4.4
bcc	[111]	4.1

should be a good indicator of whether or not $F(t)$ is sensitive to the spin value I for small t, and possibly for large t. Using this same argument, it can be seen from Eq. (20) that the largest change in line shape for a change in I should come when I is changed from $\frac{1}{2}$ to 1.

Figures 1, 3, 5, 7, 9, 11, 13, 15, 17 all show that the difference between the free induction decay shapes for $I=\frac{1}{2}$ and $I=1$ is much greater than between $I=1$ and $I=\infty$. Listed in Table I are the crystal symmetry and direction of applied magnetic field for the computed free induction decay shapes. The ranking is from the least spin-dependent (at the top) to the most spin-dependent (at the bottom) free-induction decay shape as determined by visual inspection. The third column of the table lists the corresponding values of σ which are in a monotonically decreasing sequence; therefore the smaller the dependence of $F(t)$ upon I, the larger the value of σ.

All the calculated free-induction decay curves exhibit a beat structure, some to such an extent that the corresponding calculated absorption curve is double-peaked. For the symmetries and field directions where the absorption curve is double peaked, the peaking is more pronounced for large I than for $I=\frac{1}{2}$. This is contrary to the results obtained for two particle systems and emphasizes the importance of the many particle interaction in line shape calculations.

Up to the present time there has not been published a detailed line-shape measurement or a free-induction decay measurement for a spin system in which $I=\frac{1}{2}$ and the lattice is not simple cubic, or in which $I>\frac{1}{2}$. The measurements for $I>\frac{1}{2}$ will be complicated by the quadrupole moment of the nucleus unless the crystal is extremely strain free.

APPENDIX A: EVALUATION OF $\mathrm{Tr}\{O_mO_nO_j \exp(-i\beta t) I_{jx} \exp(i\beta t)\}$

Let O_j, O_m, and O_n, be operators for the different particles j, m, and n. The three operators are not necessarily the same. Let

$$\Phi=\mathrm{Tr}\{O_mO_nO_j \exp(-(it/2\hbar)\sum_{k\neq l} B_{kl}I_{kz}I_{lz})I_{jx}\exp((it/2\hbar)\sum_{k\neq l} B_{kl}I_{kz}I_{lz})\}. \tag{A1}$$

All the terms in the exponents in Eq. (A1) commute with each other, and

$$\exp((it/2\hbar)\sum_{k\neq l} B_{kl}I_{kz}I_{lz})=\prod \exp((it/2\hbar)B_{kl}I_{kz}I_{lz}). \tag{A2}$$

Equation (A1) may be simplified by applying Eq. (A2) and passing all the exponential operators that do not contain an I_{jz} operator through the I_{jx} operator and cancelling them with the corresponding terms having the same exponent of opposite sign. Then

$$\Phi=\mathrm{Tr}\left\{O_mO_nO_j \exp\left(\frac{-itI_{jz}}{\hbar}\sum_k' B_{jk}I_{kz}\right)I_{jx}\exp\left(\frac{itI_{jz}}{\hbar}\sum_k' B_{kj}I_{kz}\right)\right\}. \tag{A3}$$

Treating the exponential operator, operating on I_{jx}, as a simple rotation operator

$$\Phi=\mathrm{Tr}\{O_mO_nO_j[I_{jx}\cos((t/\hbar)\textstyle\sum_k' B_{jk}I_{kz})+I_{jy}\sin((t/\hbar)\sum_k' B_{jk}I_{kz})]\}. \tag{A4}$$

All the traces in this paper can be reduced to this form. Two characteristic examples for the specific evaluation of Φ are given below.

For $O_m=O_n=$ unit operator and $O_j=I_{jx}$

$$\begin{aligned}\Phi&=\mathrm{Tr}\{I_{jx}^2\cos((t/\hbar)\textstyle\sum_k' B_{jk}I_{kz})+I_{jx}I_{jy}\sin((t/\hbar)\sum_k' B_{jk}I_{kz})\}\\&=\mathrm{Tr}_j\{I_{jx}^2\}\,\mathrm{Tr}_j'\{\cos((t/\hbar)\textstyle\sum_k' B_{jk}I_{kz})\}.\end{aligned} \tag{A5}$$

The second term in Eq. (A5) drops out because $\mathrm{Tr}\{I_{jx}I_{jy}\}=0$. $\mathrm{Tr}_j\{\ \}$ represents a trace only over the wave functions for the jth particle. $\mathrm{Tr}_j'\{\ \}$ represents a trace over all wave functions for all the particles except j. Thus.

$$\begin{aligned}\Phi&=\tfrac{1}{2}\,\mathrm{Tr}_j\{I_{jx}^2\}\,\mathrm{Tr}_j'\left\{\prod_k' \exp\left(\frac{itB_{jk}I_{kz}}{\hbar}\right)+\prod_k' \exp\left(\frac{-itB_{jk}I_{kz}}{\hbar}\right)\right\}\\&=\tfrac{1}{2}\,\mathrm{Tr}_j\{I_{jx}^2\}\left(\prod_k' \mathrm{Tr}_k\left\{\exp\left(\frac{itB_{jk}I_{kz}}{\hbar}\right)\right\}+\prod_k' \mathrm{Tr}_k\left\{\exp\left(\frac{-itB_{jk}I_{kz}}{\hbar}\right)\right\}\right).\end{aligned} \tag{A6}$$

Using the result that

$$\mathrm{Tr}_j\{I_{jx}^2\}=\sum_{\epsilon=-I}^{I}\epsilon^2=I(I+1)(2I+1)/3, \tag{A7}$$

and

$$\mathrm{Tr}_k\{\exp(itB_{jk}I_{kz}/\hbar)\}=\sum_{\epsilon=-I}^{I}\exp(it\epsilon B_{jk}/\hbar)=\sin((2I+1)B_{jk}t/2\hbar)/\sin(B_{jk}t/2\hbar), \tag{A8}$$

Eq. (A6) reduces to

$$\Phi=(I(I+1)(2I+1)/3)\prod_k{}'\left(\frac{\sin((2I+1)B_{jk}t/2\hbar)}{\sin(B_{jk}t/2\hbar)}\right). \tag{A9}$$

For $O_m=I_{my}^2$, $O_n=$unit operator and $O_j=I_{jx}$

$$\begin{aligned}\Phi&=\mathrm{Tr}\{I_{my}^2[I_{jx}^2\cos((t/\hbar)\textstyle\sum_k' B_{jk}I_{kz})+I_{jx}I_{jy}\sin((t/\hbar)\sum_k' B_{jk}I_{kz})]\}\\&=\tfrac{1}{2}\,\mathrm{Tr}_j\{I_{jx}^2\}\,\mathrm{Tr}_j'\left\{I_{mx}^2\left(\prod_k{}'\exp\left(\frac{itB_{jk}I_{kz}}{\hbar}\right)+\prod_k{}'\exp\left(\frac{-itB_{jk}I_{kz}}{\hbar}\right)\right)\right\}\\&=\tfrac{1}{2}\,\mathrm{Tr}_j\{I_{jx}^2\}\left(\mathrm{Tr}_m\left\{I_{mx}^2\left[\exp\left(\frac{itB_{jm}I_{mz}}{\hbar}\right)+\exp\left(\frac{-itB_{jm}I_{mz}}{\hbar}\right)\right]\right\}\right)\prod_{k\neq(j,m)}{}'\mathrm{Tr}_k\left\{\exp\left(\frac{itB_{jk}I_{kz}}{\hbar}\right)\right\}.\end{aligned} \tag{A10}$$

Since $I_{mx}=\frac{1}{2}(I_{m+}+I_{m-})$,

$$\begin{aligned}\mathrm{Tr}_m\{(I_{mx}^2\exp(itB_{jm}I_{mz}/\hbar)\}&=\tfrac{1}{4}\,\mathrm{Tr}_m\{(I_{m+}^2+I_{m+}I_{m-}+I_{m-}I_{m+}+I_{m-}^2)\exp(itB_{jm}I_{mz}/\hbar)\}\\&=\tfrac{1}{4}\,\mathrm{Tr}_m\{(I_{m+}I_{m-}+I_{m-}I_{m+})\exp(itB_{jm}I_{mz}/\hbar)\}\\&=\tfrac{1}{2}\sum_{\epsilon=-I}^{I}(I(I+1)-\epsilon^2)\exp(itB_{jm}\epsilon/\hbar)\\&=\frac{I(I+1)\sin((2I+1)B_{jk}t/2\hbar)}{2\sin(B_{jk}t/2\hbar)}+\frac{1}{2}\left(\frac{\hbar}{B_{jm}}\right)^2\frac{d^2}{dt^2}\sum_{\epsilon=-I}^{I}\exp\left(\frac{itB_{jm}\epsilon}{\hbar}\right),\\&=\frac{\sin((2I+1)B_{jk}t/2\hbar)\cos^2(B_{jk}t/2\hbar)}{4\sin^3(B_{jk}t/2\hbar)}-\frac{(2I+1)\cos((2I+1)B_{jk}t/2\hbar)\cos(B_{jk}t/2\hbar)}{4\sin^2(B_{jk}t/2\hbar)}.\end{aligned} \tag{A11}$$

Using the results of Eqs. (A7), (A8), and (A11), Φ reduces to

$$\Phi=\frac{I(I+1)(2I+1)}{12}\left(\cot^2\left(\frac{B_{jk}t}{2\hbar}\right)-(2I+1)\cot\left(\frac{B_{jk}t}{2\hbar}\right)\cot\left(\frac{(2I+1)B_{jk}t}{2\hbar}\right)\right)\prod_k{}'\left(\frac{\sin((2I+1)B_{jk}t/2\hbar)}{\sin(B_{jk}t/2\hbar)}\right). \tag{A12}$$

APPENDIX (B): CALCULATION OF $F_0(t)$

Using the result $C_0=1$, the formula for $F_0(t)$ from Eq. (11) reduces to

$$\begin{aligned}F_0(t)&=\frac{\mathrm{Tr}\{I_x\exp(i\beta t)I_x\exp(-i\beta t)\}}{\mathrm{Tr}\{I_x^2\}}\\&=\frac{\sum_{j,k}^{N,N}\mathrm{Tr}\{I_{jx}\exp((it/2\hbar)\sum_{l\neq m}B_{lm}I_{lz}I_{mz})I_{kx}\exp((-it/2\hbar)\sum_{l\neq m}B_{lm}I_{lz}I_{mz})\}}{\sum_{j,k}^{N,N}\mathrm{Tr}\{I_{jx}I_{kx}\}}.\end{aligned} \tag{B1}$$

The only nonzero traces in Eq. (B1) are those where $j=k$. Since all the operators in the exponential commute, this expression reduces to

$$F_0(t)=\frac{\sum_{j=1}^{N}\mathrm{Tr}\{I_{jx}\exp((it/\hbar)I_{jz}\sum_l' B_{jl}I_{lz})I_{jx}\exp((-it/\hbar)I_{jz}\sum_l' B_{jl}I_{lz})\}}{\sum_{j=1}^{N}\mathrm{Tr}I\{_{jx}^2\}}. \tag{B2}$$

Using the results of Appendix A, Eq. (B2) reduces to

$$F_0(t)=\sum_{j=1}^{N}\tfrac{1}{3}I(I+1)(2I+1)\prod_k{}'\left(\frac{\sin[(2I+1)B_{jk}t/2\hbar]}{\sin(B_{jk}t/2\hbar)}\right)(\tfrac{1}{3}I(I+1)(2I+1)(2I+1)^{N-1}N)^{-1}$$
$$=\frac{1}{N}\sum_{j=1}^{N}\prod_k{}'\left(\frac{\sin((2I+1)B_{jk}t/2\hbar)}{(2I+1)\sin(B_{jk}t/2\hbar)}\right). \quad \text{(B3)}$$

PHYSICAL REVIEW VOLUME 148, NUMBER 1 5 AUGUST 1966

Effects of Nonmagnetic Impurities upon Anisotropy of the Superconducting Energy Gap*

JOHN R. CLEM†
Department of Physics, University of Illinois, Urbana, Illinois
(Received 21 January 1966; revised manuscript received 5 April 1966)

The influence of the presence of nonmagnetic impurities upon the anisotropy of the superconducting energy-gap parameter is considered. Using a factorable BCS-like model for the effective electron-electron matrix element, $V_{pp'}=(1+a_p)V(1+a_{p'})$, within the context of an earlier theory by Markowitz and Kadanoff, it is shown that when impurities are present the wave-vector-dependent gap parameter Δ_p is replaced by a complex, wave-vector- and energy-dependent gap parameter $\Delta(\mathbf{p},\omega)=\Delta_i(\omega)+a_p\,\Delta_a(\omega)$. The behavior of $\Delta_i(\omega)$ and $\Delta_a(\omega)$ is extensively examined as a function of impurity concentration; it is found, for example, that the magnitude of the anisotropic part $\Delta_a(\omega)$ of the gap parameter tends to zero in the limit of large impurity concentration. A model calculation, assuming a rectangular shape for the anisotropy distribution function $P(a)$, illustrates the behavior for small and moderate impurity concentrations. The behavior for large impurity concentrations is found to depend, to lowest order, only upon the mean-squared anisotropy $\langle a^2\rangle$. The behavior of the effective density of states is also examined; it is shown to become isotropic as the impurity concentration increases. The precise shape of the effective density of states for energies near the gap is obtained for the large-impurity-concentration limit. Experimental manifestations of the reduction of the anisotropy by impurity scattering are briefly discussed.

I. INTRODUCTION

THE presence of impurities in a superconductor has an interesting influence upon the effects of anisotropy of the superconducting energy gap. An important result of the addition of ordinary nonmagnetic chemical or physical impurities is the reduction—or "washing out"—of the anisotropy of the energy gap. Such a reduction of the anisotropy has been observed in specific heat,[1–3] nuclear spin-lattice relaxation,[4] tunneling,[5] infrared absorption,[6] and surface resistance[7] experiments. Similarly, the observed initial decrease in the transition temperature as small amounts of impurities are added[8–11] is also a result of anisotropy reduction.

The theory of the reduction of anisotropy by impurity scattering, suggested by the work of Anderson,[12] has been successfully applied to the latter problem by several groups.[13–19] When impurities are present, the essential modification of the theory of the superconduct-

* Based on a thesis submitted in partial fulfillment of the requirements for the degree of Doctor of Philosophy at the University of Illinois. This research was supported in part by the Alfred P. Sloan Foundation, by the U. S. Army Research Office, Durham, under Contract No. DA-31-124-ARO(D)-114, and by the Air Force Office of Scientific Research under Contract No. AF 735-65.

† United States Steel Foundation Fellow, 1963–65. Present address: Department of Physics and Astronomy, University of Maryland, College Park, Maryland.

[1] R. Geiser and B. B. Goodman, Phys. Letters **5**, 30 (1963).
[2] B. J. C. van der Hoeven, Jr., and P. H. Keesom, Phys. Rev. **137**, A103 (1965).
[3] L. Y. L. Shen, N. M. Senozan, and N. E. Phillips, Phys. Rev. Letters **14**, 1025 (1965).
[4] Y. Masuda, Phys. Rev. **126**, 1271 (1962).
[5] P. Townsend and J. Sutton, Phys. Rev. **128**, 591 (1962); Phys. Rev. Letters **11**, 154 (1963).
[6] P. L. Richards, Phys. Letters **7**, 412 (1961).
[7] M. A. Biondi, M. P. Garfunkel, and W. A. Thompson, Phys. Rev. **136**, A1471 (1964); and in *Proceedings of The Ninth International Conference on Low Temperature Physics*, edited by J. G. Daunt, D. O. Edwards, F. J. Milford, and M. Yaqub (Plenum Press, Inc., New York, 1965), p. 387.
[8] E. A. Lynton, B. Serin, and M. Zucker, J. Phys. Chem. Solids **3**, 165 (1957).
[9] G. Chanin, E. A. Lynton, and B. Serin, Phys. Rev. **114**, 719 (1959).
[10] D. P. Seraphim, D. T. Novick, and J. D. Budnick, Acta Met. **9**, 446 (1961).
[11] D. P. Seraphim, C. Chiou, and D. J. Quinn, Acta Met. **9**, 861 (1961).
[12] P. W. Anderson, J. Phys. Chem. Solids **11**, 26 (1959).
[13] D. Markowitz and L. P. Kadanoff, Phys. Rev. **131**, 563 (1963).
[14] T. Tsuneto, Progr. Theoret. Phys. (Kyoto) **28**, 857 (1962).
[15] C. Caroli, P. G. de Gennes, and J. Matricon, J. Phys. Radium **23**, 707 (1962).
[16] M. J. Zuckermann and D. M. Brink, Phys. Letters **4**, 76 (1963).
[17] P. C. Hohenberg, Zh. Eksperim. i Teor. Fiz. **45**, 1208 (1963) [English transl.: Soviet Phys.—JETP **18**, 834 (1964)].
[18] D. M. Brink and M. J. Zuckermann, Proc. Phys. Soc. (London) **85**, 329 (1965).
[19] D. M. Ginsberg, Phys. Rev. **136**, A1167 (1964); **138**, A1409 (1965).